ISSN: 1231-4005
e-ISSN: 2354-0133
DOI: 10.5604/12314005.1213559

THEORETICAL STUDIES OF VARIABLE GEOMETRY – HOT SECTION OF THE MINIATURE JET ENGINE

Maciej Chmielewski, Szymon Fulara, Marian Gieras

Warsaw University of Technology
Institute of Heat Engineering
Nowowiejska Street 21/25, 00-665 Warsaw, Poland
tel.:+48 22 2345222
e-mail: chmielfam@wp.pl
szymon.fulara@itc.pw.edu.pl, marian.gieras@pw.edu.pl

Abstract

The aim of this article is to present the results of theoretical studies regarding the use of variable geometry hot section of a miniature gas turbine. The variable geometry combustor and variable area nozzle concepts for GTM-120 miniature jet engine are presented in particular. Recent trends of propulsion system size reduction, low-emission combustion and improved fuel efficiency have been considered. A system of variable geometry combustor and variable area nozzle has been proposed as solution.

The basic zero-dimensional analytical models for variable geometry combustor and variable area nozzle are developed. Chemkin based model shows significant NO_X/CO emissions reduction and combustor outlet enthalpy increases with the use of variable geometry combustor chamber.

The analytical model of the variable area nozzle has been proposed. It shows turbine effectiveness increase across its operating range by raising the compressor working line. As a result, noticeable turbine stage efficiency increase has been obtained.

Finally, physical implications and future work plans regarding variable geometry hot section of miniature gas turbines are discussed.

***Keywords**: small gas turbine, variable geometry, combustor chamber, turbine nozzle, efficiency*

1. Introduction

Aircraft engine design optimization is inextricably linked with the development of the aviation industry. Minimizing fuel consumption and emissions of harmful compounds has become extremely important during several last decades. This fact is reflected by International Civil Aircraft Organization (ICAO) regulations. During last 20 years, the NO_X emissions were reduced over 50% by Committee on Aviation Environmental Protection (CAEP) Tier 8 Standard.

Current lean burn technology allows meeting strict emission requirements for commercial turbofan engines. This technology however is not available for small scale and miniature jet engines used in Unmanned Aircraft Vehicles (UAVs) propulsion systems. Recent widespread use of constructions of this type in various applications including: surveillance systems, flying targets or missiles propulsion calls for low fuel consumption, operational flexibility and low emissions. It is therefore necessary to develop new technologies to meet the posed expectations.

Variable geometry hot section technology seems to be a very attractive way for engine operation optimization, especially in miniature turbine engines, where it can be limited to minor design changes. The aim of this article is to examine qualitatively and quantitatively the impact of variable geometry of the combustion chamber and turbine nozzle on performance and emissions from miniature jet engine. Basic analytical tools are used to reveal potential advantages of the use of proposed variable geometry hot section system in GTM-120 miniature jet engine.

2. Variable geometry combustor and variable area turbine nozzle

The concept of using variable geometry combustion chamber to improve the engine efficiency and reduce NO_X and CO emissions is based on primary combustion zone's equivalence ratio control. Use of the variable geometry combustor provides precise control of the amount of air supplied to each of the combustion zones: primary, intermediate and dilution. Equivalence ratio control entails the combustion temperature change, which is linked to the emission of harmful compounds (NO_X and CO). Based on [1], the ideal variable geometry system should supply larger quantities of air to the primary zone in order to lower the primary zone temperatures, thus reducing nitric oxides (NO_X) emissions, at maximum power. With a power reduction, greater part of the air shall be transferred to the dilution zone of the combustion chamber to maintain the temperature that ensures low emissions of carbon monoxide (CO). It is possible to maintain low emission levels of both NO_X and CO by keeping the primary zone temperature in the range of 1680-1900K, called low emission "window" (Fig. 1).

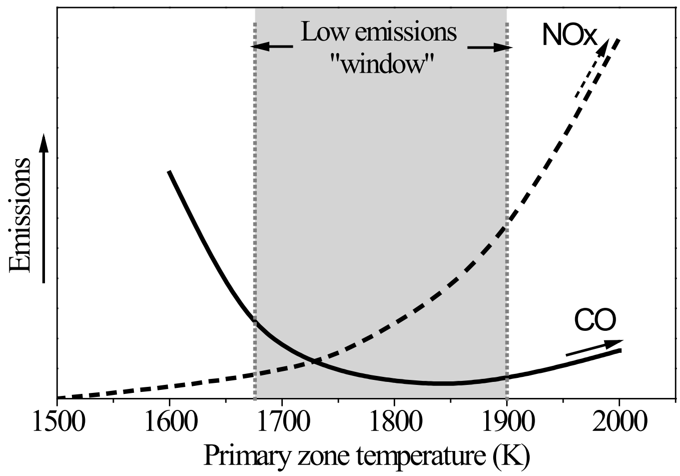

Fig. 1. Influence of primary zone temperature on CO and NO_X emissions

The variable geometry of turbine nozzle allows optimizing both: engine performance and turbine's part loads. The largest performance rise can be achieved for low turbine load. The most noticeable advantage of the Variable Nozzle Area (VAN) system can be observed for idle turbine speeds, however the significant benefits are observed below 30% of maximum gas turbine loads [2]. The variable turbine nozzle is initially controlled to decrease effective nozzle area at partial loads in order to maintain constant turbine entry temperature. Higher turbine entry temperature allows more effective energy recovery by the turbine, thus reducing specific fuel consumption (SFC) by improving compressor stall line, as shown in Fig. 2. Variable turbine nozzle closes to some point beyond which it remains in fixed position. At idle speed, the nozzle is fully open to reduce nozzle thermal stress.

An additional advantage coming from the use of variable geometry combustor and turbine nozzle is the increase in the operability range of the whole engine. Active control of the stoichiometry inside combustor primary zone leads to extension of combustion stability by extending flame blowout and flashback limits in given engine operating regime. The variable nozzle geometry can act as an active surge control system by preventing choked flow at nozzle throat.

In this article, an impact of variable geometry hot section (combustor and turbine nozzle) on miniature gas turbine performance and emissions is discussed. The theoretical studies of variable area dilution holes and variable area nozzle are performed for GTM-120 miniature gas turbine (Fig. 6). GTM-120 miniature gas turbine is designed mainly as an UAV's propulsion system. The proposed variable hot section is shown in Fig. 3. The slewing ring with series of holes matching outer liner's holes pattern is overlapping the original liner's holes reducing its area thus redistributing combustor air between primary and dilution zones. Proposed variable geometry hot section is equipped with a set of rotary nozzle airfoils located behind the combustor chamber. Rotation of the airfoils changes the airfoil's angle of attack and nozzle effective area (Fig. 4).

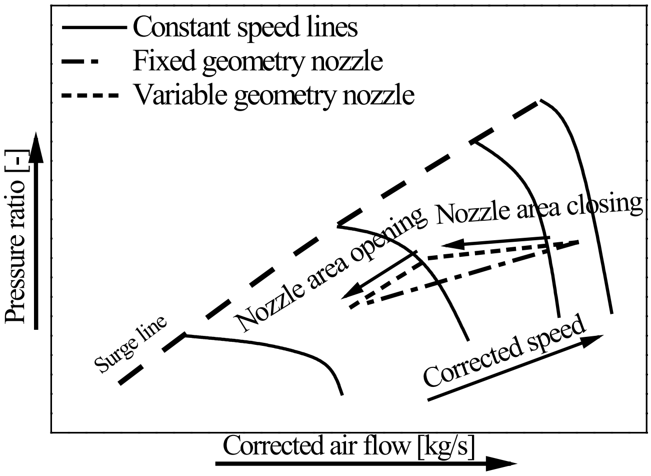

Fig. 2. Compressor working line for single spool gas turbine

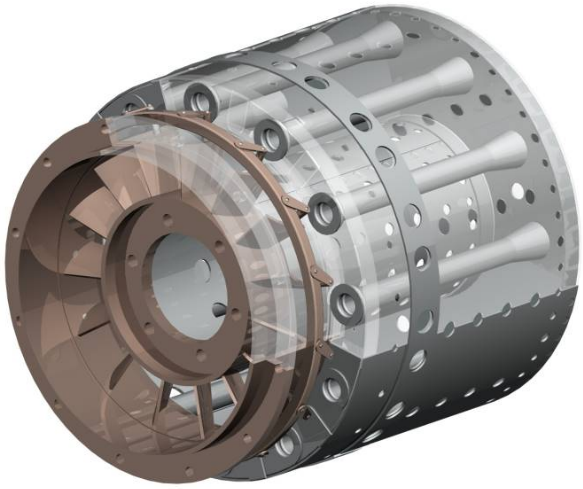

Fig. 3. Variable geometry hot section of miniature turbine engine

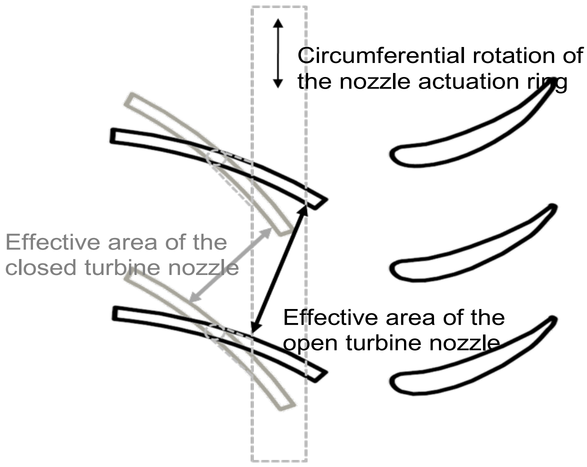

Fig. 4. Variable Area Nozzle concept

3. Analytical models for variable geometry combustor and turbine nozzle for GTM-120 miniature gas turbine

Variable geometry combustor

The basic zero-dimensional analytical model for variable geometry combustor based on combustor airflow splits is developed in this article. Subsequently the hybrid Perfectly-Stirred Reactor (PSR) – Plug-Flow Reactor (PFR) reactor network is used to study the impact of flow splits on the combustion performance and emissions.

The basic equation for flow through liner holes may be expressed as:

$$\dot{m} = C_D A_{phys} \sqrt{2\rho\left(P_{T,u} - P_{S,d}\right)}, \tag{1}$$

where:

C_D – coefficient of discharge,

A_{phys} – physical area (m^2),

ρ – gas density [kg/m^3],

$P_{T,u}$ – total pressure upstream the hole [Pa],

$P_{S,d}$ – static pressure downstream the hole [Pa].

It is assumed that total hole upstream pressure and downstream static pressure are constant, regardless of the hole position. Based on above assumption it can be stated that:

- flow through primary holes: $\dot{m}_p = 96 C_{D,p} d_p^{\,2} \varphi,$
- flow through dilution holes: $\dot{m}_d = 36 C_{D,d} d_d^{\,2} \varphi,$
- flow through vaporizing tubes: $\dot{m}_v = 12 C_{D,v} d_v^{\,2} \varphi,$

where:

d_i – diameter of i-th hole (m^2),

$\varphi = \frac{\pi}{4}\sqrt{2\rho\left(P_{T,u} - P_{S,d}\right)}$ – constant.

The coefficient of discharge for incompressible, non-swirling flow, for plain circular, oval and rectangular holes can be calculated from [3]:

$$C_D = \frac{1.25(K - 1)}{\sqrt{4K^2 - K\left(2 - \alpha\right)^2}}\cdot \tag{2}$$

For vaporizing tubes, the C_D is calculated from formula for plunged holes [4]:

$$C_D = \frac{1.65(K - 1)}{\sqrt{4K^2 - K\left(2 - \alpha\right)^2}},$$

where:

K – ratio of jet dynamic pressure to the annulus dynamic pressure upstream of the holes,

α – ratio of mass flow through the holes to mass flow through the whole annulus:

$$\alpha = \frac{\dot{m}_h}{\dot{m}_{an}}\cdot \tag{3}$$

Therefore, for the particular flow from the mass conservation law it can be written:

– for primary zone holes: $\alpha_p = \dfrac{\dot{m}_p}{\dot{m}_p + \dot{m}_d + \dot{m}_v}$,

– for dilution holes zone: $\alpha_d = \dfrac{\dot{m}_d}{\dot{m}_d + \dot{m}_v}$,

for vaporizing tubes: $\alpha_v = 1$.

Based on [5, 6] the K ratio for standard geometry of GTM-120 combustion chamber is calculated:

– for primary zone holes: $K = 4.5$,
– for dilution zone holes: $K = 3.0$,
– for vaporizing tubes: $K = 2.6$.

Direct solution for $C_{D,v}$ gives:

$$C_{D,v} = 0.534.$$

Iterative solution for $C_{D,p}$ and $C_{D,d}$ gives:

$$C_{D,p} = 0.533,$$

$$C_{D,d} = 0.530.$$

The sum of air mass flows through primary and dilution holes is equal to total engine mass flow. Five engine rotational speeds are considered in this article: 40, 60, 80, 100, 120 k rpm. Based on experimental data from GTM-120 engine bench testing [7], following mass flows are calculated:

Tab. 1. Air mass flow split in combustor and fuel consumption

Engine rotational speed (k rpm)	Air mass flow (kg/s)				Fuel consumption (g/s)
	Total	Primary zone	Dilution zone	Vaporizing tubes	
40	0.089	0.0409	0.0377	0.0105	1.58
60	0.151	0.0694	0.0639	0.0177	2.38
80	0.214	0.0983	0.0905	0.0251	3.26
100	0.274	0.1259	0.1159	0.0322	4.16
120	0.355	0.1631	0.1502	0.0417	6.34

The impact of variable geometry dilution zone hole area is calculated for four residual dilution holes areas: 90, 70, 50 and 30%. It is assumed that the coverage of dilution holes area does not impact the pressure distribution inside combustor. This is rough assumption; however, the impact of the K on discharge pressure for the considered oval holes is below 10%. The mass flow distributions for selected residual areas and engine rotational speeds are as presented in Tab. 2.

Tab. 2. Calculated mass flow splits in combustor with variable geometry: P – Primary zone, D – Dilution zone, V – Vaporizing tubes

Dilution hole residual area	90%			70%			50%			30%		
	Air mass flow (kg/s)											
Engine rotational speed (k rpm)	P	D	V	P	D	V	P	D	V	P	D	V
40	0.043	0.035	0.011	0.047	0.030	0.012	0.052	0.024	0.013	0.058	0.016	0.015
60	0.072	0.060	0.019	0.079	0.051	0.020	0.088	0.041	0.022	0.099	0.027	0.025
80	0.103	0.085	0.026	0.113	0.073	0.029	0.125	0.057	0.032	0.140	0.039	0.036
100	0.131	0.109	0.034	0.144	0.093	0.037	0.160	0.074	0.041	0.179	0.049	0.046
120	0.170	0.141	0.044	0.187	0.120	0.048	0.207	0.095	0.053	0.232	0.064	0.059

In order to study the impact of variable geometry dilution holes area on combustor performance and NOx/CO emissions the Chemkin Pro software is used. The hybrid Perfectly-Stirred Reactor (PSR) – Plug-Flow Reactor (PFR) reactor network is used to simulate mixing and flow characteristics of the gas turbine combustor (Fig. 5).

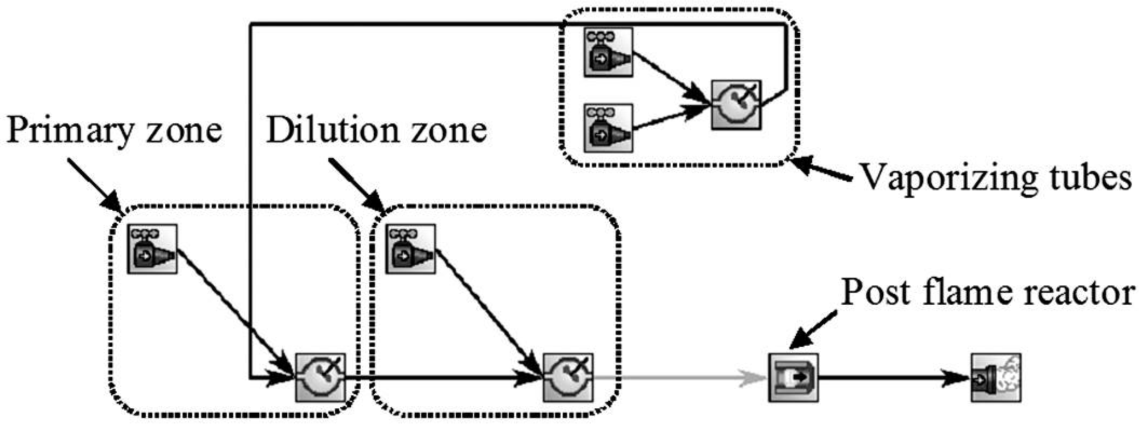

Fig. 5. Hybrid PSR–PFR reactor network

Perfectly Stirred Reactors are used to simulate mixing and reactions in vaporizing tubes, primary and secondary zones. Post flame reactor is used to simulate chemical reactions occurring in exhaust gases after combustor (turbine stage and nozzle). Residence times for each reactor and simulated engine rotational speeds are taken from CFD model presented in [5], pressures in each engine cross-sections are taken from engine test bench [7] (Fig. 6). Volume of each reactor is calculated based on 3-D CAD model supplied by engine manufacturing company – JETPOL. The air is modelled as 79% mole fraction of N_2 and 21% mole fraction of O_2.

The kerosene combustion is modelled with a reduced kinetic mechanism developed for high temperature combustion of Jet-A [8]. Mechanism uses mixture of 72.7% n-decane, 9.1% of n-hexane and 18.2 % of benzene as a kerosene surrogate. Reduced mechanism includes 38 reactions and does not account for NOx production, therefore it was supplemented with NO and NO_2 production mechanisms (reactions 39-46) from [9] (Tab. 3).

Tab. 3. Supplement NO_x production mechanism and rate constants (units: cm^3-mole-s-cal-K)

No	Reaction	A	n	E_a
39	$N+O_2$<=>$NO+O$	9.00E+09	1.000	6500
40	$N+NO$<=>N_2+O	2.70E13	0.000	355
41	$N+OH$<=>$NO+H$	3.360E+13	0.000	385
42	$N_2O(+M)$<=>$N_2+O(+M)$	7.910E+10	0.000	56020
43	N_2O+O<=>$2NO$	2.900E+13	0.000	23150
44	N_2O+O<=>N_2+O_2	1.400E+12	0.000	10810
45	NO_2+O<=>$NO+O_2$	3.900E+12	0.000	-240
46	HO_2+NO<=>NO_2+OH	2.110E+12	0.000	-480

Reaction mechanisms (39-41) are thermal NO (the extended Zeldovich mechanism), (42-44) is NO formation from N_2O at higher pressures and mechanism (45) is NO_2 reduction to NO at high temperatures and (46) is NO to NO_2 mechanism. Both mechanisms have negative activation energy. As the temperature decreases, the rate of this reaction increases.

Variable geometry turbine nozzle

The optimum turbine nozzle is usually designed taking into account three main design features: specific rotational speed (usually at cruise condition); turbine nozzle inlet temperature (limited by material and cooling) and required compressor shaft rotational speed and torque.

Below a basic analytical model of the variable area nozzle is presented. It is based on standard analytical methods of calculating optimum turbine nozzle for today's engine [10-13]. Authors aimed to optimize the geometry for specified turbine rotational speeds by adjusting the nozzle inlet angle and thus changing the effective nozzle area. The basic iteration has been performed in order to determine the right parameters and equations describing turbine flow through the turbine stage of variable nozzle geometry.

The calculations start with basic expression describing turbine effective work:

$$l_T = \Delta h_{Tiz} \cdot \eta_T \,, \tag{4}$$

where:

Δh_{Tiz} – turbine isentropic enthalpy,

η_T – turbine thermal efficiency.

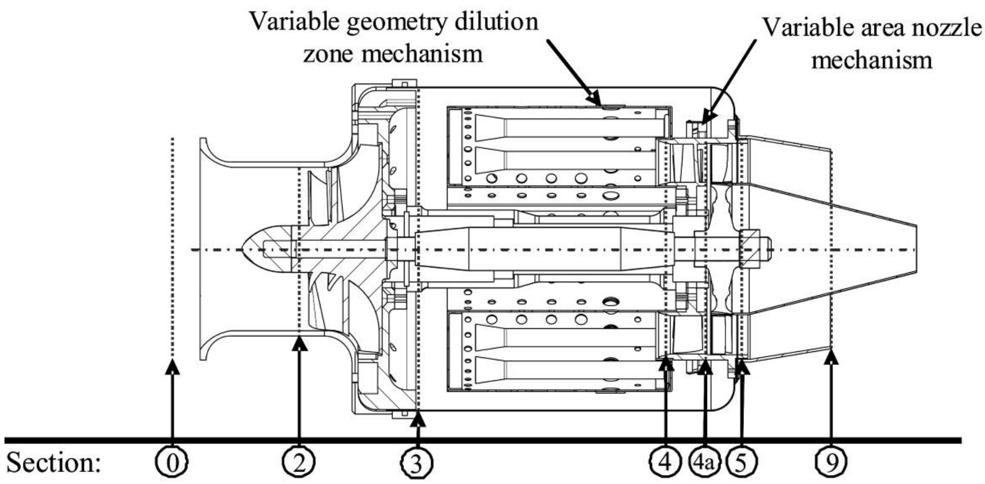

Fig. 6. Section numbering on the miniature jet engine. Variable geometry of hot section is visible

The l_T, turbine effective labour, is calculated using theoretical, isentropic enthalpy loss and thermodynamic efficiency. The isentropic enthalpy loss is a parameter that has been derived based on general knowledge of turbine design and thermodynamic properties. The amount of enthalpy loss has been calculated at 100 kJ/kg level. The isentropic enthalpy loss is a difference between the inlet temperature and turbine outlet isentropic expansion temperature multiplied by specific heat of working medium at constant pressure.

The basic notion of turbine velocity triangles is shown in Fig 7.

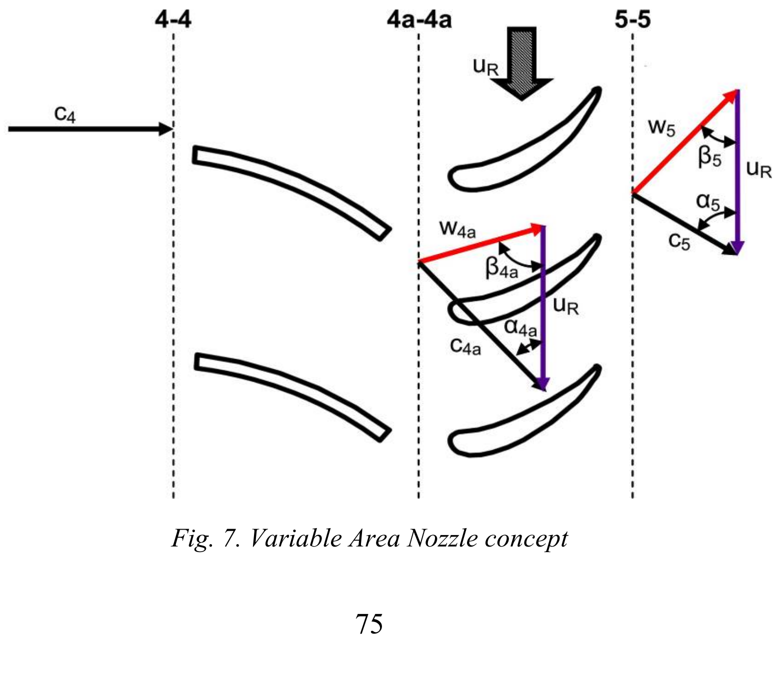

Fig. 7. Variable Area Nozzle concept

The combustion gases thermodynamic parameters at nozzle and rotor outlets are calculated using standard equations:

$$T_{ia} = T_i^* - \frac{c_{ia}^2 \cdot (k_s - 1)}{2 \cdot k_s R_s}, \tag{5}$$

$$p_{ia} = p_i^* \left(1 - \frac{c_{ia}^2 \cdot (k_s - 1)}{2 \cdot \varphi^2 k_s R_s T_i^*}\right)^{\frac{k_s - 1}{k_s}}, \tag{6}$$

where i – index of selected cross-section (4a and 5 respectively).

Most of the parameters used in above expressions are presented in Tab. 4. The other like c_{ia}, the absolute velocity at turbine nozzle outlet, have been derived using standard expressions for velocity triangles and airfoil geometry.

Next step involves calculations of the geometrical parameters of turbine nozzle. The velocity triangles (Fig. 7) are used to derive formulae for nozzle outlet velocity and nozzle outlet low angle. Based on assumed geometrical parameters of the rotor blades, the rotor inlet angle has been calculated leading to derivation of rotor outlet velocity, rotor outlet flow angle and rotor rotational speed.

In addition, the temperature and pressure have been calculated at given sections (sections 4, 4a and 5). In the end, the efficiency of the turbine is calculated using the following formula:

$$\eta_T = \frac{u_R(w_{4a} \cos\beta_{4a} + w_5 \cos\beta_5)}{\Delta h_{Tiz}} \left(1 - \xi_\delta - \xi_f - \xi_s\right) \eta_{mech}.$$

Several assumptions are made during the iteration procedure. The most important parameters are listed in Tab. 4. Iterations have been carried out to fit η_T assumed at the beginning of the procedure and calculated at the end to check if the algorithm works.

Tab. 4. Turbine nozzle and rotors parameters

Parameter	**Symbol**	**Value**	**Source**
Average turbine diameter	D_t	0.1 [m]	measurements
Turbine rotational velocity	N	40-120 [x1000 rpm]	measurements
Nozzle loss coefficient	Φ	96 [%]	[12]
Tip clearance loss coefficient	H	95 [%]	[12]
Circumferential to absolute velocity ratio	$\frac{u_R}{c_3}$	0.8-1.2 [-]	calculated
Nozzle inlet absolute pressure	P_4^*	108.5-212.9 [kPa]	measurements
Nozzle inlet absolute temperature	T_4^*	860-990 [K]	measurements
Nozzle inlet angle	α_{4a}	15-25 [deg]	given
Rotor loss coefficient	Ψ	97 [%]	[12]
Heat capacity ratio	k_s	1.33 [kJ/kg·K]	-
Specific gas constant	R_s	287 [kJ/kg·K]	-
Circumferential to absolute isentropic velocity ratio	$\frac{u_R}{c_{ais}}$	0.60 [-]	calculated
Tip clearance loss coefficient	ξ_δ	0.02 [-]	[12]
Blade tip rub loss coefficient	ξ_f	0.01 [-]	[12]
Sealing loss coefficient	ξ_s	0.005 [-]	[12]
Mechanical efficiency	η_{mech}	0.995 [-]	[12]

4. Results

As a result of calculations performed for variable geometry combustor, the 3-D combustor performance maps were obtained: NO_X emissions (Fig. 8a), CO emissions (Fig. 8b) and combustor outlet temperature (Fig. 8c). Fig. 8c indicates that minimum exhaust gas temperature is obtained for maximum dilution holes area and lowest engine speed corresponding to lowest engine power. As expected, more cooling air directed to dilution zone has an adverse effect on the NO_X emission level (Fig. 8a). This behaviour is maintained throughout the engine rotational speed range. Based on above maps it is possible to calculate emission per power unit, therefore creating optimum control law for low NO_X emissions.

For CO emission, it can be observed that minimum emissions are obtained for around 80k rpm rotational speeds. This behaviour is in accordance with relation shown in Fig. 1. For 80k rpm the optimal primary zone equivalence ratio (thus temperature) is obtained, resulting in minimum CO emissions. Moreover, it can be noticed that reduction of dilution hole area results in increasing CO production. This is because of additional cooling air near liner walls, which is supplied into primary combustion zone with reduction of dilution holes area. The temperature of this near wall air is low enough to reduce effectively chemical reaction responsible for removing CO at lower temperatures:

$$CO + H_2O \Leftrightarrow CO_2 + H_2 .$$

It is worth noticing that NO_X emissions obtained by basic zero-dimensional analytical model presented in this article are in good agreement with experimental results described in [7]. Presented CO emissions are overestimated, however the trends are equivalent to those obtained in [7] with minimum emissions for 80k rpm. The combustor outlet temperatures are also overestimated but with trends corresponding to engine test bench results. Observed discrepancies from experimental data can be explained by simplicity of analytical model. Basic model presented in the paper, as mentioned, does not include heat transfer effects. The engine is treated adiabatically, which may contribute to excessive combustor outlet temperatures. Reduced kinetic mechanism utilized in Chemkin software due to the limited number of chemical reaction equations may not fully indulge species concentrations and combustion temperatures. It is deemed that use of detailed combustion kinetic mechanisms may contribute to more accurate species concentrations and temperatures predictions.

The results of proposed variable geometry turbine nozzle analytical model calculations have been presented in the form of 3-D turbine performance maps. Turbine exit temperature is presented on Fig. 8a and the turbine outlet pressure is shown in Fig. 5b.

One can notice that both, the exit temperature and outlet pressure are decreasing with the nozzle angle increase. The temperature and pressure decrease are directly linked to the turbine efficiency. The bigger temperature and pressure decrease on the turbine stage, the more efficient is the system. Exit parameters decrease is directly linked to the nozzle angle change, which directly affects the nozzle exit flow velocity and indirectly – flow velocity at the turbine exit.

The nozzle exit flow velocity cannot increase infinitely. It is limited by chocked flow condition. The chocking condition describes the dependence of flow on speed of sound. When the flow through turbine reaches the speed of sound then the drag coefficient becomes significant. The miniature gas turbine must not reach the speed of sound neither on nozzle nor on the rotor side. The general formula (1) defines the pressure ratio at which the flow reaches sonic condition. For k = 1.33 the formula returns 0.54.

$$\frac{p_i{}^*}{p_{ia}} = \left(\frac{2}{k+1}\right)^{\frac{k}{k-1}}, \tag{7}$$

where:

i – index of selected cross-section (4 and 4a respectively).

Above this value, the flow is choked. Turbine nozzles are actually designed to reach sonic flow at cruise. In addition, minor exceeding of the barrier of sound at nozzle airfoil tip may be desired from the turbine efficiency perspective. At cruise speed turbine works close to the sonic values in the nozzle throat. Locally the barrier of sound may be exceeded. The pressure ratio at the smallest effective nozzle area and at the nozzle outlet becomes critical. The expansion waves arise at the end of the convex side of the airfoil. The geometry of the nozzle guarantees efficient energy recovery and may improve system reliability.

The presented model shows that the turbine efficiency may be improved at high rotational speeds by nozzle angle adjustment. The higher rotational speed, the higher improvement may be achieved.

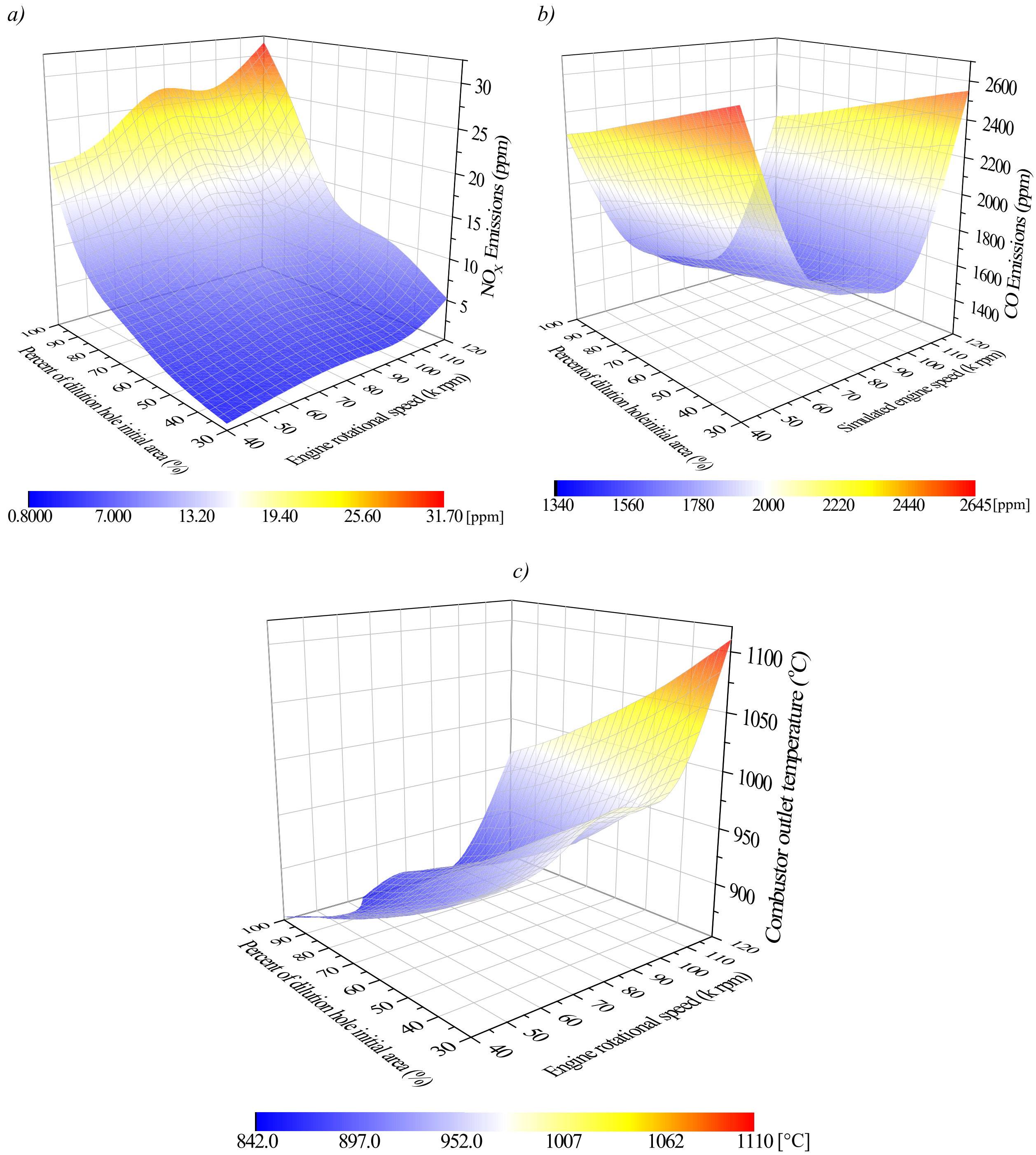

Fig. 8. 3-D combustor performance maps: NO_x Emissions, b) CO Emissions, c) Combustor outlet temperature

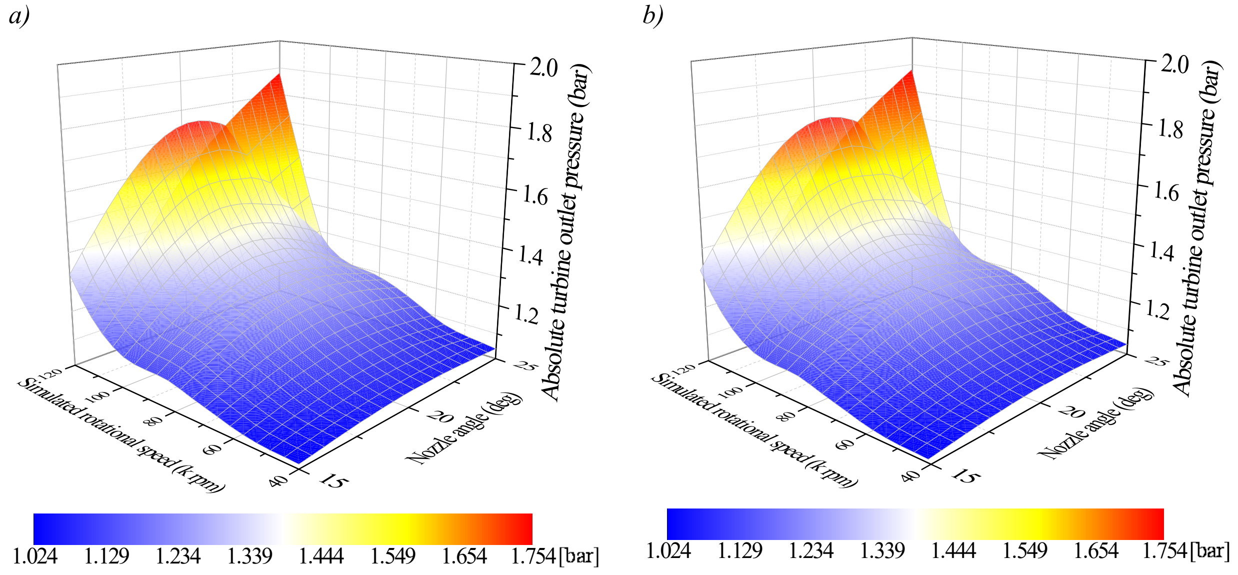

Fig. 9. 3-D turbine performance maps: Temperature after turbine stage, b) Absolute turbine outlet pressure

5. Conclusions

This article presents a theoretical study of the use of variable geometry combustion chamber and turbine nozzle in a miniature turbine engine. The concept of variable cross-section area dilution holes and variable angle turbine nozzle for use in GTM-120 engine has been developed and presented. The zero- and one-dimensional analytical models have been developed in order to evaluate the impact of the hot section geometry changes on performance and emissions from the engine.

The results obtained with the developed models are in good agreement with emissions, temperatures and pressures after turbine stage measurements. The temperatures at the combustor outlet section are somewhat overestimated by the analytical model. Adiabatic combustor modelling is identified as a main source of discrepancies between proposed model and real engine measurements. Predictions of the NO_X emissions are within 15% accuracy to experimental data [7], which is very good estimation for such simplified chemical reactions modelling. The CO emissions are within 37% accuracy to experimental data [7]. It is important to notice that simple one-dimensional modelling results of combustor performance should be treated as qualitative, not quantitative model due to 1-D limitations. Presented results show the benefits of the utilization of the proposed variable geometry concept in a miniature gas turbine. Significant improvement over standard engine performance and reduction of NO_X emissions can be obtained with the use of variable geometry. Up to 75% reduction in NO_X emissions can be obtained according to the proposed model. Up to 125°C combustor, outlet temperature can be achieved. Increase of the combustor outlet enthalpy results in the increase of the overall thermal efficiency. Additionally, impact on the CO emissions is shown (decreasing the outlet combustor temperatures leads to increase of CO emissions). The calculations were performed for a miniature gas turbine; however, some of the results may also be applicable to the full-scale gas turbine engine. The use of variable geometry hot section may also entail some disadvantages, which are:

- Increase in the engine's weight and price,
- Adverse influence on engine's maintainability,
- Reliability decrease due to increased complexity.

Current, fixed, combustor and turbine nozzles designs are reaching their performance limits. Variable geometry hot section is very promising idea for further effectiveness increase across completely operating range of the gas turbine engines. Increase in the turbine inlet temperature leads to increase in turbofan engine thrust and decrease of Specific Fuel Consumption (SFC). During most of the engine missions, it operates below the maximum allowable turbine inlet temperature (limited by material properties). The temperature may be adjusted with the use Variable Area Nozzle. Such system controls the gas temperature by changing the nozzle effective area. Basic calculations showed 15% improvement in turbine efficiency for 120k rpm.

The concept, however, has to face many real life issues. The turbine rotational speed is limited by rotor durability. Moreover, the Variable Nozzle Area design requires vane tip clearances control system in order to account for various turbine-operating conditions. An active Clearance Control (ACC) system should be used in order to guarantee improved efficiency in comparison to fixed-geometry turbine. A combined system of variable nozzle and simultaneous active clearance control would significantly improve turbine engine performance.

Engines of improved performance and reduced emissions are the future of civil and military aviation in the mid and short term. They will allow improving the affordability and endurance of propulsion systems.

6. Future work

Authors built the miniature turbine engine test stand and designed variable geometry combustor and turbine nozzle. Basic analytic model is going to be refined with 3-D Computational Fluid Dynamic modelling with detailed chemistry kinetics modelling. Transient effects are to be included in the refined model. Experimental results obtained on the test stand are going to be used to verify applicability and correctness of models used. Finally, obtained results are going to be used to prove the legitimacy of use of the variable geometry hot section in small gas turbines.

References

[1] Lefebvre, A. H., Ballal, D. R., *Gas Turbine Combustion: Alternative Fuels and Emissions*, CRC Press, Boca Raton, 2010.

[2] Welsh, P., Fletcher, P., *Gas Turbine Performance*, Blackwell Science Ltd, Oxford 2004.

[3] Kaddah, K. S., *Discharge Coefficients and Jet Deflection Angles for Combustor Liner Air Entry Holes*, College of Aeronautics MSc thesis, Cranfield, UK 1964.

[4] Freeman, B. C., *Discharge Coefficients of Combustion Chamber Dilution Holes*, College of Aeronautics MSc thesis, Cranfield, UK 1965.

[5] Gieras, M., Stańkowski, T., *Computational study of an aerodynamic flow through a micro-turbine engine combustor*, Journal of Power Technologies 92 (2) pp. 68-79, Warsaw 2012.

[6] Ślesik, D., *Numeryczna symulacja aerodynamiki przepływu przez komorę spalania silnika GTM-120*, Praca dyplomowa inżynierska, Warsaw 2011.

[7] Chmielewski, M., Gieras, M., *Small Gas Turbine GTM-120 Bench Testing with Emission Measurements,* Journal of KONES, Vol. 22(1), 2015.

[8] Strelkova, M. I., Kirillov, I. A., Potapkin, B. V., Safonov, A. A., Sukhanov, L. P., Umanskiy S. Ya. , Deminsky M. A., Dean A. J., Varatharajan B., Tentner A. M., *Detailed and Reduced Mechanisms of Jet-A Combustion at High Temperatures*, Combustion Science and Technology, Vol. 180: pp 1788-1802, 2008.

[9] Smith, G. P., Golden, D. M., Frenklach, M., Moriarty, N. W., Eiteneer, B., Goldenberg, M., Bowman, C. T., Hanson, R. K., Song, S., Gardiner, W. C., Jr., Lissianski, V. V., Qin, Z., http://www.me.berkeley.edu/gri_mech/

[10] Mattingly, J. D., W. H. Heiser, D. T. Pratt, *Aircraft engine design*, AIAA, Reston 2002.

[11] Mattingly, J. D., *Elements of propulsion: Gas turbines and rockets*, AIAA, Reston 2006.

[12] Szczeciński, S., *Turbinowe napędy samochodowe*, Wyd. Komunikacji i Łączności, Warsaw 1974.

[13] Tuliszka, E., *Turbiny cieplne*, Wyd. Naukowo-techniczne, Warsaw 1973.